UCRL-JRNL-221904

LAWRENCE
LIVERMORE
NATIONAL
LABORATORY

Identification of external influences on temperatures in California

C. Bonfils , P. Duffy, B. Santer, T. Wigley, D. Lobell, T. Phillips, C. Doutriaux

June 9, 2006

Climatic Change

shortened title: Temperatures in California

Identification of external influences on temperatures in California

Céline Bonfils[1], Philip B. Duffy[2,1], Benjamin D. Santer[2], Tom M. L. Wigley[3],
David B. Lobell[2], Thomas J. Phillips[2], Charles Doutriaux[2]
[1]University of California, Merced, California
[2]Lawrence Livermore National Laboratory, Livermore, California
[3]National Center for Atmospheric Research, Boulder, Colorado

Corresponding author: Céline Bonfils
Lawrence Livermore National Laboratory
P.O. Box 808 L-103
Livermore, CA 94550
Tel: (925) 423-9923/ Fax: (925) 423-4908
Email: bonfils2@llnl.gov

submitted: 06/01/06

This work was performed under the auspices of the U.S. Department of Energy by University of California, Lawrence Livermore National Laboratory under Contract W-7405-Eng-48.

Abstract: We use eight different observational datasets to estimate California-average temperature trends over 1950-1999. Observed results are compared to trends from a suite of control simulations of natural internal climate variability. Observed increases in annual-mean surface temperature are distinguishable from climate noise in some but not all observational datasets. The most robust results are large positive trends in mean and maximum daily temperatures in late winter/early spring, as well as increases in minimum daily temperatures from January to September. These trends are inconsistent with model-based estimates of natural internal climate variability, and thus require one or more external forcing agents to be explained. Our results suggest that the warming of Californian winters over the second half of the twentieth century is associated with human-induced changes in large-scale atmospheric circulation. We also hypothesize that the lack of a detectable increase in summertime maximum temperature arises from a cooling associated with large-scale irrigation. This cooling may have, until now, counteracted the warming induced by increasing greenhouse gases and urbanization effects.

1. Introduction

Human-induced climate change is a reality. Human effects on climate have been identified in many different aspects of the climate system, at global, hemispheric (*e.g.*, Santer *et al.*, 1996; Mitchell *et al.*, 2001; Hegerl *et al.*, 1997; Tett *et al.*, 1999; Stott *et al.*, 2000) and continental scales (Stott, 2003; Zwiers and Zhang, 2003; Karoly *et al.*, 2003; Karoly and Braganza, 2005). Attempts to detect anthropogenic effects at regional or even grid-point scales are more recent (Spagnoli *et al.*, 2002, Santer *et al.*, 2006, Karoly and Wu, 2005). In California, there is great political and scientific interest in the question of how human-caused climate change will manifest itself. Will nighttime temperatures increase more than daytime temperatures? Will there be more warming in winter than in summer? How will precipitation and snow be affected? How uncertain are expected changes? Impacts on agriculture, water availability, human health, *etc*. depend on answers to these and related questions.

Identification of "fingerprints" of anthropogenic climate change at the scale of California would enhance confidence in model projections of the regional aspects of climate change and their possible societal impacts. Part of such fingerprinting work consists in documenting the background 'noise' of natural internal climate variability and determining whether or not observed trends are too rapid to be explained by this noise alone. It is impossible to determine noise characteristics from short instrumental records in which signals and noise convolved, but natural internal variability can be estimated from long climate model control simulations with no changes in external factors.

Attribution is the more difficult problem of identifying causal factors responsible for any detected change. Rigorous attribution of observed changes in Californian climate to specific forcings would require so-called "single forcing" experiments, simulating changes in only one forcing at a time. These were not available for a broad range of climate models. Hence, we instead consider "20CEN" experiments driven by historical changes in combined anthropogenic and natural external forcings, and then determine if these forced simulations yield results consistent with observed changes. Consistency between the observed and 20CEN climate changes (and inconsistency between the observed changes and control run results) would imply that we have detected significant changes in Californian climate, and can attribute these changes to external forcing(s). Inconsistencies would point towards errors in (or neglect of) important forcings, and/or errors in the model response to the imposed forcings.

In small domains, detection of externally-forced climate change poses special challenges. Global models are less skillful on sub-continental scales (Stott and Tett, 1998), and high-resolution observational datasets are not always available. Furthermore, the noise of internal climate variability generally increases with decreasing domain size, often leading to a degradation of signal-to-noise (S/N) ratios, and hampering identification of external factors. Finally, forcings that may be of considerable importance in understanding regional climate change (*e.g.*, land-use change, aerosols) are spatially and temporally heterogeneous and uncertain.

We focus on indices of Californian climate based on daily surface air temperatures: monthly-mean temperature (T_{ave}), monthly-mean night- and day-time temperatures (T_{min}, T_{max}) and their difference, the diurnal temperature range (DTR). All are well observed in California, and their changes can have important societal impacts. We consider both seasonal and annual mean trends in these indices.

2. Data and Methods

Observed California-mean trends in each quantity are estimated for 1950-1999 from a minimum of four and a maximum of seven gridded datasets (Table 1), as well as from stations of the U.S. Historical Climatology Network (USHCN). Use of multiple datasets allows us to assess the robustness of our detection results to observational uncertainty. For example, version 1 of the University of Washington temperature dataset (UW1) is less suitable for long-term trend analysis than version UW2, which includes adjustments for non-climatic influences (*e.g.*, changes in instrumentation and station location; Hamlet and Lettenmaier, 2005). USHCN observations, also adjusted for inhomogeneities (Karl *et al.*, 1990), have been widely used for trend and long-term variability analyses in California. Although the datasets analyzed here rely on similar raw data and are not completely independent, the processing choices made by dataset developers can differ markedly from group to group, leading to uncertainty in the magnitude (and sometimes even the sign) of the observed trends (see Figures 1 and 2).

In Section 3, we investigate if observed historical trends in California exceed climate 'noise' by comparing recent observed 50-year trends in T_{ave}, T_{min}, T_{max}, and DTR to trends from 22 (for T_{ave}) or 6 (for T_{min}, T_{max}, and DTR) long, control simulations (Karoly *et al.*, 2003; Santer *et al.*, 2006) performed in support of the IPCC Fourth Assessment Report (AR4, Table 2). For each run, we fitted least-squares linear trends to overlapping 50-year segments (separated by 10-year intervals) of the California-average temperature time series. Trends from the 22 (6) models were then combined, yielding a multi-model distribution of 808 (137) unforced 50-year trends for each climate variable. These distributions reflect noise uncertainties arising from differences in a wide range of model properties (physics, parameterizations, resolution, *etc.*), and provide the best available model estimates of natural internal variability. The significance of observed trends was assessed in two ways: 1) by comparing observed trends with the 95% confidence intervals of the trend distributions, computed by assuming a Gaussian distribution of trends and multiplying the standard error of the distribution (s_E) by 1.96; 2) by determining the empirical probability that the magnitude of the unforced trends exceeds that of observed trends. The two methods give very similar results, validating the assumption of the Gaussian distribution of trends (Figure 3). While none of the control runs has a statistically significant overall temperature trend for the Californian domain, some integrations do show residual drift at the beginning of the run (Santer *et al.*, 2006). We opted to retain these control-run drifts, thus inflating s_E and making it more difficult to reject the null hypothesis that an observed trend is due to natural internal variability.

The significance-testing procedure outlined above was applied to annual- and seasonal-mean [January-March (JFM), April-June (AMJ), July-September (JAS), and October-December (OND)] values of the four indices considered here. We used this somewhat unconventional seasonal definition because observed trends in December are very different from those in January (see below). We also compare observed trends to those from 69 (15) 20CEN realizations performed with 22 (8) different models (Table 2).

The reliability of the significance-testing results depends crucially on the fidelity with which the models used here simulate the natural internal variability of the real-world climate system. This is difficult to assess, particularly on the 50-year timescales of interest here, without multi-century observational records uncontaminated by human influences. However, observational data are of adequate length to make meaningful comparisons of modeled and observed temperature variability on annual and decadal timescales (*e.g.* Stott, 2003; Braganza *et al.*, 2004). Accurate simulation of natural variability on these shorter time scales would enhance our confidence in the detection results for 50-year trends. We compared the observed interannual and decadal variability of each temperature index with corresponding values from the 20CEN realizations. The (varying) length of the observational record dictated the period used for calculating model and observed temporal standard deviations. All standard deviations were computed after first removing the overall linear trend from the area-average data, which constitutes a zero-order estimate of the influence of external forcing. The interannual variability is simply the standard deviation of the residuals. The decadal standard deviation is computed after low-pass filtering the regression residuals with a Lynch and Huang (1992) digital filter with half-power at a period of 119 months (Santer *et al.*, 2006). The results of this variability comparison are discussed in Section 4.

3. Results of detection analysis

All gridded observational datasets show a consistent pattern of increasing annual-mean temperatures and decreasing annual-mean DTR over most of California. Over most California, trends have a high degree of purely statistical significance (Figures 1 and 2). Similar results are found for the USHCN station data. Such consistency across multiple datasets increases our confidence in the reality of these annual-mean T_{ave} and DTR changes. Annual-mean T_{ave} increased by 0.36 to 0.92°C over 1950-1999, depending on the observational dataset considered. Three of the eight observed trends (for USHCN, UW2, and CRU2.0) are significant different from internal climate variability at the 95% or greater confidence level (Figure 3). T_{ave} changes are largest in wintertime and are significant in all eight observational datasets. This strongly suggests that external forcing(s) are required to explain the observed JFM trends in T_{ave}. Two datasets (USHCN and UW2) have significant T_{ave} trends in spring. No observational dataset yields significant T_{ave} trends in summer or fall.

This analysis of daily-mean temperatures masks interesting information in the diurnal cycle of temperature change. Substantial night-time warming occurs in every month except in December (not shown), and trends in T_{min} are inconsistent with internally-generated climate noise in every season except OND (Figure 3b). In contrast, monthly trends in observed daily maximum temperatures exceed estimated internal variability only in late winter/early spring (Figure 3c), with largest warming in January and March (1.5°C over 50 years), slower rate of warming in February (0.5°C over 50 years) and cooling in December. Observed trends in DTR exceed the estimated noise during summer only (Figure 3d), reflecting the much greater increase in minimum temperature than in maximum temperature in those months.

We consider next whether observed changes in California temperature indices are consistent with results from 20CEN simulations with combined anthropogenic and natural forcings (Table 2). In general, the models fail to reproduce the observed seasonality of changes in T_{ave}, T_{min}, T_{max}, and DTR (Figure 4, lower panels). While most simulations capture the observed JAS trends in T_{ave}, T_{min}, and T_{max} (but not DTR), they tend to underestimate the observed JFM trends in T_{ave}, T_{min}, and T_{max}.

Such deficiencies in the simulation of regional trends are not surprising, and have a number of possible explanations. First, many of the 20CEN runs examined here do not incorporate changes in spatially- and temporally heterogeneous forcings like land use, carbonaceous aerosols, indirect aerosol effects, *etc.* (Santer *et al.*, 2006). These forcings have probably made significant contributions to regional-scale climate change. Second, even models that include some representation of heterogeneous and highly uncertain forcings may lack the spatial resolution to reliably represent the climate response to the imposed forcings: the entire state of California is represented by a minimum of 5 and maximum of 35 grid-boxes in the AR4 models analyzed here. Finally, comparison of multiple 20CEN realizations performed with the same model reveal that individual realizations can have very different 50-year trends. Reliable estimation of the true response to the imposed forcing changes may require larger ensemble sizes than were available in the IPCC AR4 database (Table 2).

4. Discussion

Karoly *et al.* (2003) performed a detection analysis similar to ours, focusing on land surface temperature changes over North America (between 30N° to 65°N). They found that the increase in annual-mean surface air temperature of roughly 0.65°C from 1950 to 1999 (in HadCRUT2v) could not be explained by natural internal variability. Our results for California also show an annual mean T_{ave} increase in three datasets that is significantly larger than control run noise, but not in HadCRUT2v (Figure 3). However, while Karoly *et al.* reported an observed DTR decrease that was indistinguishable from control-run noise, we obtained significant annual-mean DTR decreases in two of five observational datasets.

Our conclusion that external factors are perturbing the climate in California depends on the reliability of the model-based noise estimates. As discussed above, it is ot possible to evaluate the simulations of noise on the relevant (50-yr) time scale; nonetheless, our confidence in the finding that many of the observed trends cannot be explained by climate noise would be diminished if the models systematically underestimate noise on interannual and decadal timescales. There is no evidence that this is the case (Figure 4, top panels). For T_{ave}, while Stott and Tett (1998) found that 1990s-era models generally underestimated climate variability at spatial scales below 2000 km, none of the AR4 models has internanual variability below the lower end of the range of observational estimates, and only two models (GISS-ER and MRI-CGCM2.3.2) systematically underestimate the decadal variability (*i.e.*, each 20CEN realization lies below the observational range). The fact that most AR4 models do not underestimate decadal variability increases confidence in our model-based estimates of longer-timescale climate noise, but does not rule out systematic errors in those estimates. For T_{min}, T_{max}, and DTR indices, fewer observational datasets and simulations are available. None of the models examined here systematically underestimates the magnitude of decadal variability for either T_{min} or T_{max}. Interannual and decadal variability in DTR is however systematically underestimated by three models, suggesting that T_{min} and T_{max} covariability is too high in these models, while these indices are more decoupled in other models and in the observations.

Finer-resolution simulations with relevant forcings should improve our ability to reproduce the seasonality of observed trends. With appropriate simulations unavailable, researchers have resorted to exploratory explanations of observed temperature trends in California. For example, Christy *et al.* (2006), using their own observational temperature dataset, reported rapid night-time warming in the Central Valley over 1910 to 2003, but not in surrounding mountains. They attribute this warming to the effects of large-scale irrigation (an interpretation questioned by Bonfils *et al.* (2006)), but do not identify the physical mechanism responsible for the change. Bereket *et al.* (2005) attribute night-time warming in the Valley to increased population, urbanization, and road construction. None of these mechanisms, however, explains the pronounced seasonal variations in temperature trends.

In JFM, observed trends in T_{min}, T_{max} and T_{ave} are unlikely to be explained by natural internal variability alone. A larger JFM warming trend is consistent with a stronger snow-albedo feedback in this season, but the spatial pattern of the observed warming does not clearly support this interpretation. A more plausible explanation is that a trend towards warmer California winters is associated with a long-term change in large-scale atmospheric circulation over the North Pacific Ocean. This change is characterized by a southward shift of wind fields over the central North Pacific and a northward shift over the west coast of North America (Dettinger and Cayan, 1994, their Figure 10d). Analysis of trends in NCEP-50 observed JAS 700 mb height anomalies reveals that the circulation-change patterns identified by Dettinger and Cayan are very pronounced in January and March (months characterized by robust detection in trends of T_{min}, T_{max} and T_{ave}), with a concurrent warming in coastal sea surface temperatures. This circulation change is less pronounced in February and is qualitatively different in December, consistent with observed temperature trends. The results of other studies suggest us that greenhouse-gas forcing is likely to be implicated in this seasonal circulation shift. First, Zwiers and Zhang (2003) found that the combined effects of greenhouse gas and sulfate aerosol forcing caused significant North American warming in wintertime only. Then, Shindell *et al.* (2001) linked increasing greenhouse gas concentrations with increased flow of warm air from the Pacific Ocean to western North America, consistent with Dettinger and Cayan's analysis. Finally, Gillett *et al.* (2005) detected an anthropogenic signal in DJF sea-level pressure trends over 1948-1998, with a coherent decrease over the North Pacific and an increase over the west coast of North America, features that coincide with those noted by Dettinger and Cayan. Gillett *et al.* also found that models underestimate this circulation change, which may explain why the rise in JFM T_{ave} in the AR4 simulations is weaker than in observations (Figure 4, lower panel).

In summer, the externally-forced trend towards warmer nights is captured by at least one realization of every model (except for the single realization of BCCR-BCM2.0). However, most models overestimate the daytime warming (which is weak in the observations, and not separated from the noise). Consequently, significant changes in DTR are not reproduced by the models. One interpretation of this result is that the 20CEN simulations neglect an important regional forcing. An obvious candidate is irrigation, which is widely employed in California, and is generally not represented in 20CEN simulations performed with global models. Although the effect of irrigation on night-time temperature remains uncertain, irrigation causes day-time evaporative cooling (Lobell *et al.*, 2006; Kueppers *et al.*, 2006). At the global scale, the much smaller annual-mean increase in T_{min} than in T_{max} (Karl *et al.*, 1993) is not captured by global models. This may be due to either an absence of a significant cloudiness trend that is present in observations (Braganza *et al.*, 2004) or to the lack of prognostic photosynthesis in most global models (Bonfils *et al.*, 2004). In the Central Valley, summertime cloudiness is probably too low to be implicated in explaining differential T_{min} and T_{max} trends. Irrigation is a more credible hypothesis, and appears consistent with the observed cooling of summer days and warming of summer nights in the Central Valley, and day- and night-time warming elsewhere. In summary, the JAS trends in Figure 3 can be interpreted in several ways. One explanation is that trends in T_{max} over California are due to natural climate fluctuations alone. A more plausible interpretation (in view of the large temporal changes in irrigation in the Central Valley, the likely physical impacts of these changes, and their absence in 20CEN simulations) is that irrigation-induced cooling of T_{max} has obscured a warming signal arising from the combined effects of greenhouse gases and urbanization.

5. Conclusions

We show that external forcing(s) are perturbing the climate of California in certain seasons. The domain size is smaller than that used in most previous regional-scale detection studies. However, by employing multiple observational and model datasets, we gained confidence in both the robustness of the observed signals and their detection relative to model noise estimates. We hypothesize that the rise in late winter/early spring temperatures (T_{ave}, T_{min}, T_{max}) is associated with long-term changes in large-scale atmospheric circulation that are human-induced. It is also likely that the lack of a significant T_{max} trend in summer reflects a partial offsetting of the positive radiative effects of greenhouse gases and urbanization by the negative radiative effects of irrigation. More work is needed to solidify these findings.

One implication of our findings is that anthropogenic forcings may be more readily detectable in regional-scale ocean surface temperature changes (Santer *et al.*, 2006), than in regional-scale land-surface temperature changes with current simulations. The latter are more strongly influenced by local factors, such as land-use, topography, and urbanization. High-resolution, multi-decadal transient simulations of the effects of individual forcings would help to characterize the regional signatures of these forcings. Such simulations have not been performed to date, in part due to computational limitations, and in part because reliable information on the forcings themselves is not always available (*e.g.*, detailed descriptions of historical land-use patterns). Finally, in the case of forcings like aerosols, there are still significant uncertainties in both our understanding of their climatic effects and our ability to correctly model these effects. Nevertheless, our study represents a credible first step towards the identification and physical interpretation of the effects of external forcings on Californian climate.

Acknowledgments

This work was supported by the State of California through the Public Interest Energy Research Program. We acknowledge the modeling groups for providing data for analysis, and PCMDI for collecting and archiving the model data. The IPCC Data Archive at Lawrence Livermore National

Laboratory is supported by the Office of Science, U.S. Department of Energy. The USHCN dataset was developed and is maintained at the National Climatic Data Center (NCDC) and the Carbon Dioxide Information and Analysis Center (CDIAC) of Oak Ridge National Laboratory. NCEP Reanalysis and UD data were provided by the NOAA-CIRES Climate Diagnostics Center, Boulder, Colorado, USA, via their web site http://www.cdc.noaa.gov/. HadCRUT2v, CRU2.0 and CRU2.1 were provided by the Climatic Research Unit (http://www.cru.uea.ac.uk/cru/data/).The NOAA (National Oceanic and Atmospheric Administration) dataset was produced by the Global Climate Perspectives System (GCPS) and obtained from the NCDC. UW1 and UW2 meteorological data were obtained from the Surface Water Modeling group at the University of Washington via the web site at http://www.hydro.washington.edu/Lettenmaier/gridded_data.

References

Braganza, K., Karoly, D. J., and Arblaster, J. M.: 2004, 'Diurnal temperature range as an index of global climate change during the twentieth century', *Geophys. Res. Lett.*, **31**, L13217, DOI: 10.1029/2004GL019998.

Bereket, L., Fabris, D., Gonzalez, J. E., Chiappari, S., Zarantonello, S., Miller, N. L., and Bornstein, R.: 2005, 'Urban heat islands in California's Central Valley', *Bull. Am. Meteorol. Soc., **86***, 1542–1543.

Bonfils, C., Duffy, P. B., and Lobell, D. B.: 2006, 'Comment on 'Methodology and Results of Calculating Central California Surface Temperature Trends: Evidence of a Human-Induced Climate Change?'', *J. Clim.*, submitted.

Bonfils, C., Fung, I., Doney, S., and John, J.: 2004, 'On the detection of summertime terrestrial photosynthetic variability from its atmospheric signature', *Geophys. Res. Lett.*, **31**, L09207, DOI: 10.1029/2004GL019453.

Christy, J. R., Norris, W. B., Redmond, K., and Gallo, K. P.: 2006, 'Methodology and Results of Calculating Central California Surface Temperature Trends: Evidence of a Human-Induced Climate Change?', *J. Clim.,* **19**, 548–563.

Dettinger, M. D., and Cayan, D. R.: 1994, 'Large-scale atmospheric forcing of recent trends toward early snowmelt runoff in California', *J. Clim.*, **8**, 606–623.

Eischeid, J. K., Baker, C. B., Karl, T. R., and Diaz, H. F.: 1995, 'The quality control of long-term climatological data using objective data analysis', *J. Appl. Meteor.*, **34**, 2787–2795.

Gillett, N. P., Allan, R. J., and Ansell, T. J.: 2005, 'Detection of external influence on sea level pressure with a multi-model ensemble', *Geophys. Res. Lett.*, **32**, L19714, DOI: 10.1029/2005GL023640.

Hamlet, A. F., and Lettenmaier, D. P.: 2005, 'Production of temporally consistent gridded precipitation and temperature fields for the continental U.S.', *J. Hydrometeorology,* **6**, 330–336.

Hegerl, G. C., Hasselmann, K., Cubasch, U., Mitchell, J. F. B., Roeckner, E., Voss, R., and Waszkewitz, J.: 1997, 'Multi-fingerprint detection and attribution analysis of greenhouse gas, greenhouse gas-plus-aerosol and solar forced climate change', *Clim. Dyn.*, **13**, 613–634.

Jones, P. D., and Moberg, A.: 2003, 'Hemispheric and large-scale surface air temperature variations: An extensive revision and an update to 2001', *J. Clim.*, **16**, 206–223.

Karl, T. R., Jones, P. D., Knight, R. W., Kukla, G., Plummer, N., Razuvayev, V., Gallo, K. P., Lindesay, J., Charlson, R. J., and Peterson, T. C.: 1993, 'A new perspective on recent global warming--Asymmetric trends of daily maximum and minimum temperatures', *Bull. Amer. Meteor. Soc.,* **74***,* 1007–1023.

Karl, T. R., Williams, C. N. Jr., and Quinlan, F. T.: 1990, 'U.S. Historical Climatology Network (HCN) Serial Temperature and Precipitation Data', ORNL/CDIAC-30, NDP-019/R1. Carbon Dioxide Information Analysis Center, Oak Ridge National Laboratory, U.S. Department of Energy, Oak Ridge, Tennessee.

Karoly, D. J., and Braganza, K.: 2005, 'A new approach to detection of anthropogenic temperature changes in the Australian region', *Meteorol. Atmos. Phys*., **89**, 57-67.

Karoly, D. J., Braganza, K., Stott, P. A., Arblaster, J. M., Meehl, G. A., Broccoli, A. J., and Dixon, K. W.: 2003, 'Detection of a human influence on North American climate', *Science*, **302**, 1200–1203.

Kueppers, L. M., Snyder, M. A., Sloan, L. C., Cayan, D., Jin, J., Kanamaru, H., Kanamitsu, M., Miller, N. L., Tyree, M., Du, H., and Weare, B.: 2006, 'Multi-model comparison of the climate response to land-use change in the western United States', *Glob. Planet. Change*, submitted.

Lobell, D., Bala, G., and Duffy, P. B.: 2006, 'Biogeophysical impacts of cropland management on climate', *Geophys. Res. Lett*., (in press).

Lynch, P., and Huang, X. -Y.: 1992, 'Initialization of the Hirlam model using a digital-filter', *Mon. Weath. Rev.*, **120**, 1019–1034.

Maurer, E. P., Wood, A. W., Adam, J. C., Lettenmaier, D. P., and Nijssen, B.:2002, 'A Long-Term Hydrologically-Based Data Set of Land Surface Fluxes and States for the Conterminous United States', *J. Clim.,* **15**, 3237–3251.

Mitchell, J. F. B., Karoly, D. J., Hegerl, G. C., Zwiers, F. W., Allen, M. R., and Marengo, J.: 2001, 'Detection of climate change and attribution of causes', *Climate Change 2001: The Scientific Basis, Contribution of Working Group I to the Third Assessment Report of the Intergovernmental Panel on Climate Change,* J. T. Houghton et al., Eds., Cambridge University Press, Cambridge, pp. 695–738.

Mitchell, T. D., Carter, T. R., Jones, P. D., Hulme, M., and New, M.: 2004, 'A comprehensive set of high-resolution grids of monthly climate for Europe and the globe: the observed record (1901–2000) and 16 scenarios (2001–2100)', Tyndall Working Paper 55, Tyndall Centre, UEA, Norwich, UK. http://www.tyndall.ac.uk/.

Mitchell, T. D., and Jones, P. D.: 2005, 'An improved method of constructing a database of monthly climate observations and associated high-resolution grids', *Int. J. Climatol.*, **25**, 693–712.

Santer, B. D., Taylor, K. E., Wigley, T. M. L., Johns, T. C., Jones, P. D., Karoly, D. J., Mitchell, J. F. B., Oort, A. H., Penner, J. E., Ramaswamy, V., Schwarzkopf, M. D., Stouffer, R. J., and Tett, S.: 1996, 'A search for human influences on the thermal structure of the atmosphere', *Nature,* **382***,* 39–46.

Santer, B. D., Wigley, T. M. L., Boyle, J. S., Gaffen, D. J., Hnilo, J. J., Nychka, D., Parker, D. E., and Taylor, K. E.: 1999, 'Statistical significance of trends and trend differences in layer-average atmospheric temperature time series', *J. Geophys. Res.*, **105**, 7337–7356.

Santer, B. D., Wigley, T. M. L., Gleckler, P. J., Bonfils, C., Wehner, M. F. AchutaRao, K., Barnett, T. P., Boyle, J. S., Bruggemann, W., Fiorino, M., Gillett, N., Hansen, J. E., Jones, P. D., Klein, S. A., Meehl, G. A., Raper, S. C. B., Reynolds, R. W., Taylor, K. E., and Washington, W. M.: 2006, 'Causes of ocean surface temperature changes in Atlantic and Pacific hurricane formation regions', *Proc. Nat. Acad. Sci.*, submitted.

Shindell, D. T., Schmidt, G. A., Miller, R. L., and Rind, D.: 2001, 'Northern Hemisphere winter climate response to greenhouse gas, ozone, solar, and volcanic forcing', *J. Geophys. Res.*, **106**, 7193–7210.

Spagnoli, B., Planton, S., Deque, M., Mestre, O. and Moisselin, J. -M.: 2002, 'Detecting climate change at a regional scale: The case of France', *Geophys. Res. Lett.,* **29**, DOI: 10.1029/2001GL014619.

Stott, P. A.: 2003, 'Attribution of regional-scale temperature changes to anthropogenic and natural causes', *Geophys. Res. Lett.* **30**, DOI: 10.1029/2003GL017324.

Stott, P. A., and Tett, S. F. B.: 1998, 'Scale-Dependent Detection of Climate Change', *J. Clim.,* **11**, 3282–3294.

Stott, P. A., Tett, S. F. B., Jones, G. S., Allen, M. R., Mitchell, J. F. B., and Jenkins, G. J.: 2000, 'External control of 20th century temperature by natural and anthropogenic forcings', *Science*, **290**, 2133–2137.

Tett, S. F. B., Stott, P. A., Allen, M. R., Ingram, W. J., and Mitchell, J. F. B.: 1999, 'Causes of twentieth-century temperature change near the Earth's surface', *Nature*, **399**, 569–572.

Willmott, C.J., and Matsuura, K.: 1998, 'Global Air Temperature and Precipitation: Regridded Monthly and Annual Climatologies (version 2.01)', Newark, Delaware: Center for Climatic Research, Dept. of Geography, Univ. of Delaware.

Zwiers, F.W. and Zhang, X.: 2003, 'Towards regional climate change detection', *J. Clim.*, **16**, 793–797.

Figure and Table legends

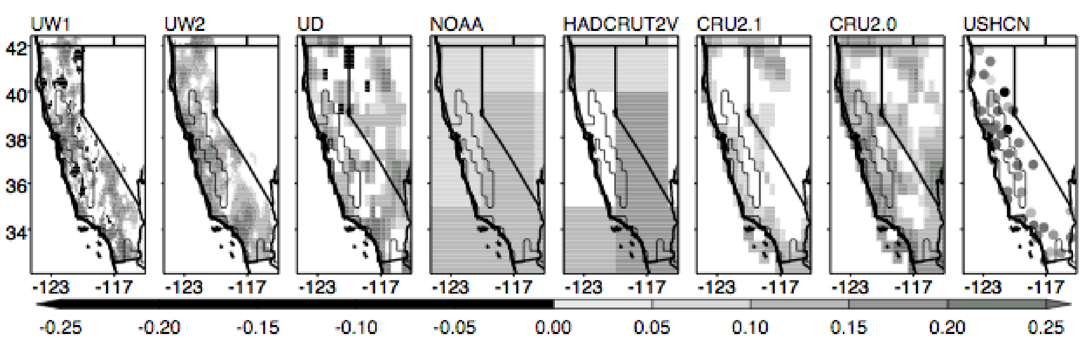

Figure 1: Spatial patterns of annual-mean temperature trends (°C/decade) in different observational datasets. At each grid-cell, trends were estimated by a least-squares linear fit to times series of temperature anomalies over 1950-1999. Trends that are not

statistically different from zero at the 80% confidence level are in white. The 150 meter contour roughly delineates California's Central Valley.

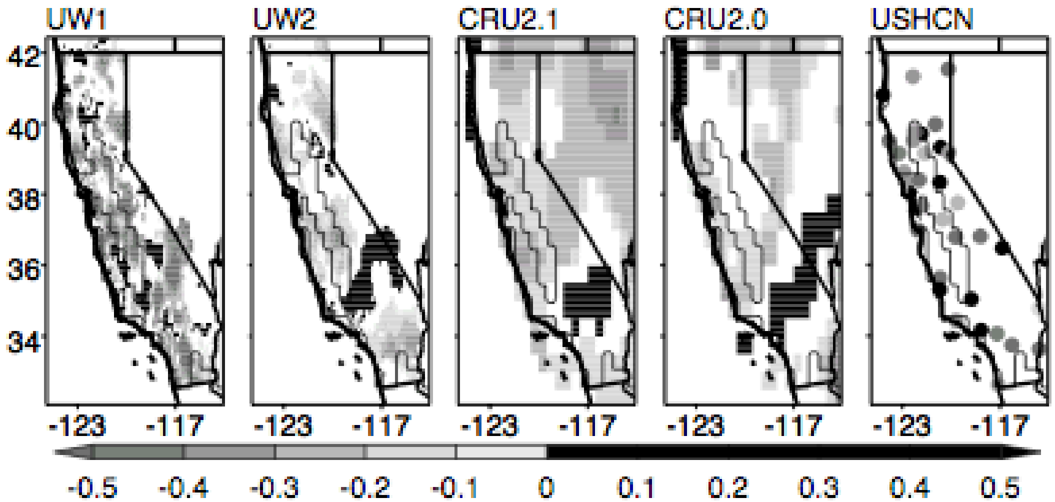

Figure 2: As for Figure 1, but for trends in diurnal temperature range.

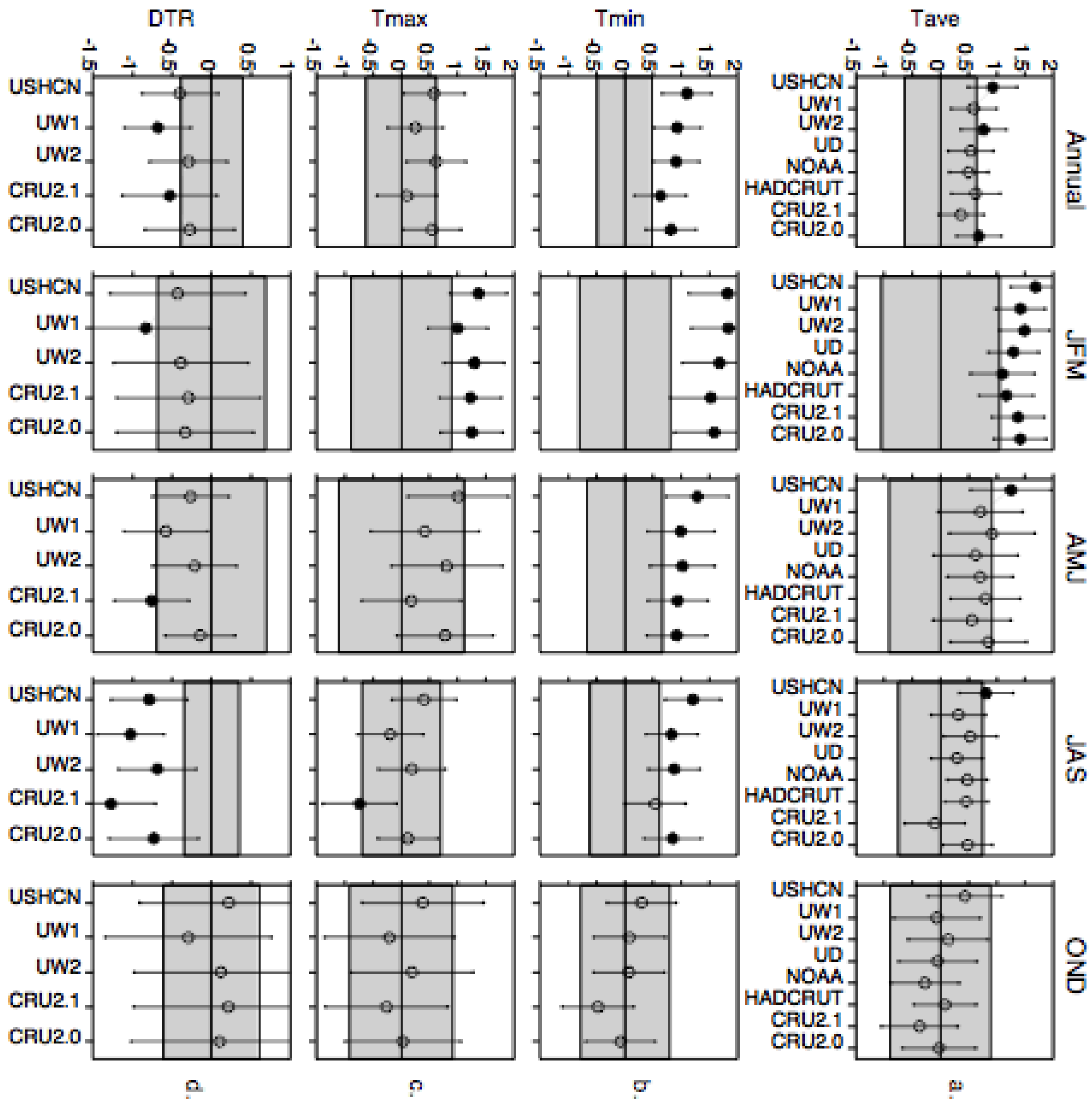

Figure 3: Observed temperature trends (solid dots) and model-derived estimates of the 95% confidence interval natural internal variability. Model results are based on multi-model trend distributions (see main text). The horizontal dotted lines are 1.96 × s_E, the standard error of the sampling distribution of unforced trends. Results are for (a) daily-mean temperature; (b) daily minimum temperature; (c) daily maximum temperature; (d) diurnal temperature range. Vertical bars represent the standard error for the trend accounting for the temporal autocorrelation of the regression residuals (Santer *et al.*, 1999) × 1.641 to assess the statistical significance of the trends (one-tailed t-test). Circles are closed when the empirical probability for the magnitude of the unforced trends to exceed that of observed trends is less than 5%. Data from different USHCN stations are equally weighted.

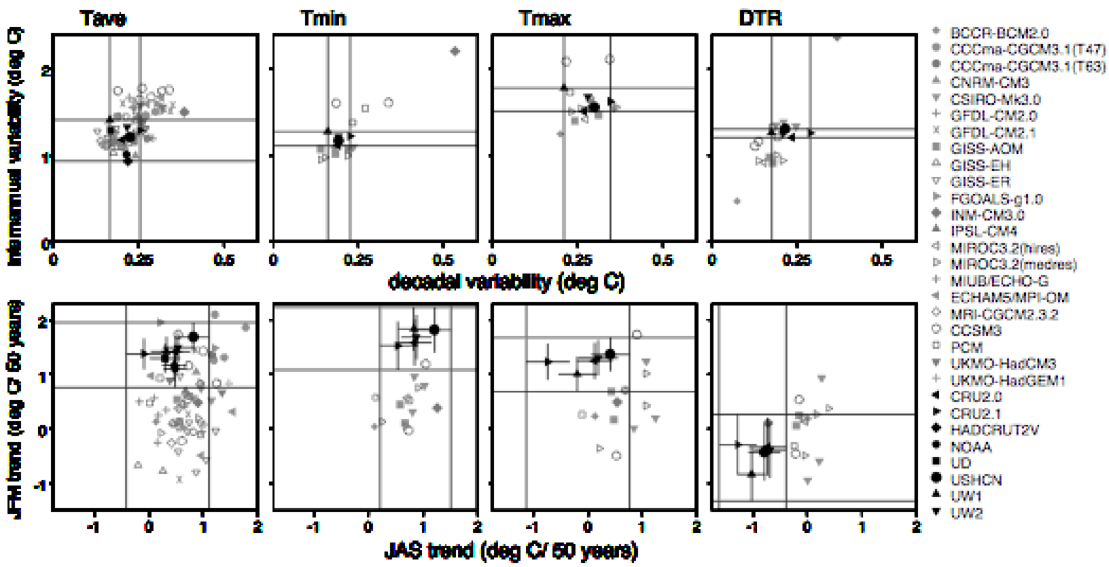

Figure 4: Comparison of statistical properties of four simulated and observed temperature indices in California. Upper panels: standard deviations of filtered and unfiltered anomaly data for 1915-1999 (except for UW2, UW1 and UD, see text). Lower panels: 1950-1999 trends in summer (JAS) and winter (JFM). Observational data sets are in black and include a 1σ trend confidence interval adjusted for temporal autocorrelation effects. Individual realizations from 22 global climate models are in grey. Vertical and horizontal lines denote the minimum and maximum observed values, and facilitate comparison with model results.

Table 1: Observational data sets, including their spatial and temporal resolution.

Acronym	Affiliation	Period*	Region	Res	Tave	Tmin	Tmax	DTR	Reference
UW1	University Washington	1949-1999	U.S.	1/8º	Y	Y	Y	Y	Maurer *et al.* (2002)
UW2	University Washington	1915-2003	West U.S.	1/8º	Y	Y	Y	Y	Hamlet and Lettenmaier (2005)
UDv1.02	University Delaware	1950-1999	Global	1/2º	Y	-	-	-	Willmott and Matsuura (1998)
NOAA	NOAA NCDC	1851-2000	Global	5º	Y	-	-	-	Eischeid *et al.* (1995)
HadCRUT2v	Hadley Center	1856-2003	Global	5º	Y	-	-	-	Jones and Moberg (2003)
CRU2.0	University East Anglia	1901-2000	Global	1/2º	Y	Y	Y	Y	Mitchell et al. (2004)
CRU2.1	University East Anglia	1901-2002	Global	1/2º	Y	Y	Y	Y	Mitchell and Jones (2005)
USHCN	Oak Ridge Nat. Lab.	variable	U.S.	N/A	Y	Y	Y	Y	Karl et al. (1990)

* in complete years

Table 2: Characteristics of 20th century climate simulations and their associated models and included external forcings that were used to estimate natural internal climate variability. See PCMDI web site (http://www-pcmdi.llnl.gov for more details).

Model Designation	Resolution	Originating group(s)	R_a	R_b	Forcings	Y_1	Y_N	L	N_a	N_b
CCSM3	T85	NCAR, USA	6	2	ABCEFJK	280	509	230	19	–
GFDL-CM2.0	2.0 × 2.5°	GFDL, USA	3	–	ABCEFIJK	1	500	500	46	–
GFDL-CM2.1	2.0 × 2.5°	GFDL, USA	3	–	ABCEFIJK	1	500	500	46	–
GISS-EH	4.0 × 5.0°	GISS, USA	5	–	ABCDEFGHIJ	188	227	400	36	–
GISS-ER	4.0 × 5.0°	GISS, USA	9	–	ABCDEFGHIJ	190	240	500	46	–
MIROC3.2(medres)	T42	CCSR/NIES/FRCGC, Japan	3	3	ABCEFGHIJK	230	279	500	46	46
MIROC3.2(hires)	T106	CCSR/NIES/FRCGC, Japan	1	1	ABCEFGHIJK	1	100	100	6	6
MIUB/ECHO-G	T30	MIUB/METRI/MD	5	–	ACDJK	186	220	341	30	–
MRI-CGCM2.3.2	T42	MRI, Japan	5	–	ACJK	185	220	350	31	–
PCM	T42	NCAR, USA	4	2	ABCJK	451	107	629	58	–
UKMO-HadGEM1	1.25 ×1.87°	UKMO, UK	2	–	ABCDEFIJK	192	209	172	13	–
BCCR-BCM2.0	T63	BCCR, Norway	1	1	AC	185	209	250	21	21
CCCma-CGCM3.1(T47)	T47	CCCma, Canada	5	–	AC	185	285	100	96	–
CCCma-CGCM3.1(T63)	T63	CCCma, Canada	1	–	AC	185	219	350	31	–
CNRM-CM3	T63	CNRM, France	1	–	ABCE	193	242	500	46	–
CSIRO-Mk3.0	T63	CSIRO, Australia	3	3	AC	187	225	380	34	34
ECHAM5/MPI-OM	T63	MPI, Germany	3	–	ABCD	215	265	506	46	–
FGOALS-g1.0	T42	LASG/IAP, China	3	–	AC	185	219	350	31	–
GISS-AOM	3.0 × 4.0°	GISS, USA	2	2	ACH	185	210	251	21	21
INM-CM3.0	4.0 × 5.0°	INM, Russia	1	1	ACJ	187	220	330	29	9
IPSL-CM4	2.5 × 3.75°	IPSL, France	1	–	ACD	186	235	500	46	–
UKMO-HadCM3	2.5 × 3.75°	UKMO, UK	2	–	ABCD	185	220	342	30	–
TOTAL	–		69	15	–	–	–	–	80	13

Ra, R_b: number of 20th century climate realizations available for Tave and for Tmin, Tmax.
Forcing used in the 20th century runs (Santer *et al*., 2006): A: Greenhouse gases, B: Ozone, C: sulfate aerosol direct effects, D: sulfate aerosol indirect effects, E: black carbon, F: organic carbon, G: mineral dust, H: sea salt, I: land-use change, J: Solar Irradiance, K: volcanic aerosols.
Y_1, Y_N, L: model-specific choices for the starting year, the ending year, and the length (in years) of the control runs.
N_a, N_b: number of overlapping 50-year linear trends obtained from each control run for Tave and for Tmin, Tmax, DTR (when data are supplied).